TWO-DIMENSIONAL TEMPERATURE RETRIEVAL IN BIOLOGICAL STRUCTURES BY MULTIFREQUENCY MICROWAVE RADIOMETRY: A SOBOLEV-SPACE SOLUTION

Fernando Bardati, Valerie J. Brown and Piero Tognolatti

Dipartimento di Ingegneria Elettronica,
Tor Vergata University of Rome, Italy

Abstract

The problem of retrieving a two-dimensional temperature distribution from radiometric data measured at various frequencies and for different positions of the sensing antenna around the body has been considered. The retrieval has been modelled as an inverse problem whose solution is investigated in a suitably defined functional space which takes regularity properties of temperature functions into account. The retrieval of hot spots in a cylinder at uniform temperature has been numerically analyzed, the examples being relevant in the hyperthermia treatment of malignancies.

1. Introduction

Anti-tumoral hyperthermia is the application of heat to malignant cells as an adjuvant of radiotherapy and chemotherapy in cancer treatment. The monitoring and control of the temperature distribution, in an anatomic area heated during a hyperthermia session, are important aspects of treatments. Subcutaneous tissue temperatures are currently measured by inserting thermocouples or optical sensors. Drawbacks of these types of sensors exist and motivate an exploration of non-invasive methods of measurement. Among non-invasive methods different approaches have been studied. Multispectral microwave radiometry has been considered [Miyakawa, 1981; Bardati and Solimini, 1983; Chivé *et al*, 1984; Mizushina *et al*, 1986; Bocquet *et al*, 1986] as being the only technique which measures the temperature directly, while other non-invasive techniques measure variations with temperature of physical quantities other than temperature.

Due to the strong attenuation of microwaves in high-water-content tissues, a microwave radiometer supplies data proportional to the average temperature in a tissue region up to a depth of 3-4 cm from the body surface. The average is weighted by a "weighting function" which takes into account (a) the morphology and dielectric properties of the tissue surrounding the antenna, (b) the frequency band of microwave receiver, and (c) the response of the contacting antenna used to receive the radiation. Properly, the antenna behaves as a transducer from fluctuating temperature-dependent electromagnetic radiation inside tissue to fluctuating electrical currents in the radiometer input device. Since the weighting function depends on frequency, the fine structure of the temperature can be obtained, in principle, by elaborating the data of radiometric measurements performed at different frequencies. The theoretical problem of the temperature reconstruction inside bodies of simple shapes (homogeneous and layered half-spaces) has received attention in the past. The retrieval has been modeled as the solution of a Fredholm integral equation of the first kind whose kernel is the weighting function. This inverse problem is an ill-posed one: the solution is not stable with respect to small variations of the data (noise). Therefore, only a finite number of components of the solution with respect to a suitable basis can be accurately determined. The appropriate basis is provided by the singular system of the integral operator [Bardati *et al*, 1987; Bardati and Brown, 1991 a].

In a recent paper [Bardati *et al*, 1991 b] it has been shown that the retrieval of temperature can considerably benefit from some *a priori* information on regularity properties of the function to be retrieved. The function space of physical temperatures has been assumed to be the space of continuous *thermal* functions. The latter have been defined as solutions of a steady-state heat-transfer equation together with an homogeneous Dirichlet condition on the boundary of the observed region. The computations, which have been carried out for the case of radiometric

observation of a homogeneous circular cylinder, show an improvement of retrievals with respect to previous reconstructions. However, closed-form expressions of thermal functions are readily obtained only for very simple structures. In this paper we consider the extension of the method to include cylinders whose electromagnetic and thermal behaviour is characterized by nonuniform parameters, therefore requiring a numerical approach. The data are simulated by letting the radiometric antenna sense the surface of a circular cylinder along a circle on a plane normal to the axis. In this way a two-dimensional inverse problem is generated, that is, the temperature is retrieved as a function of depth (i.e., in the direction from surface inwards) and in the transversal direction (along the scanning line).

2. Two-dimensional radiometer equation

Let us denote by Ω the cross-section of the cylindrical body, normal to the cylinder axis (z-axis). The antenna is modeled as a truncated parallel-plate waveguide Γ, width w, whose aperture lies on a plane α which is secant to the boundary, $\partial\Omega$, of Ω at points P_α, $P_{\alpha'}$ (Fig.1). Let P be intermediate between P_α, and $P_{\alpha'}$. In the following $P(\phi)$ will identify the measurement point around the body, where ϕ is the polar angle in the fixed frame x,y. It is worth noting that a living tissue body undergoes a small deformation caused by the pressure of the contacting antenna, which is filled by a solid dielectric material in most practical situations. For the sake of simplicity, this deformation is accounted for in our model by cutting away $\Gamma \cup \Omega$.

The dependence of the radiometric datum, T_a, on the physical temperature T(P') at a point $P' \in \Omega$ is given by the radiometric equation

$$T_a(P,\nu) = \int_\Omega W(P,P',\nu)\, T(P')\, dP' \tag{1}$$

where ν is frequency and Ω is a non-negative weighting function normalised according to

$$\int_\Omega W(P,P',\nu)\, dP' = 1 \quad . \tag{2}$$

T_a is called the available radiometric temperature of the source, when the latter is observed through the antenna at position P.

Equation (1) defines a mapping from an object space of functions of $P' \in \Omega$ into an image space of functions of ϕ and ν. In practice, only a discrete set of data is given, corresponding to radiometric data measured at M positions,

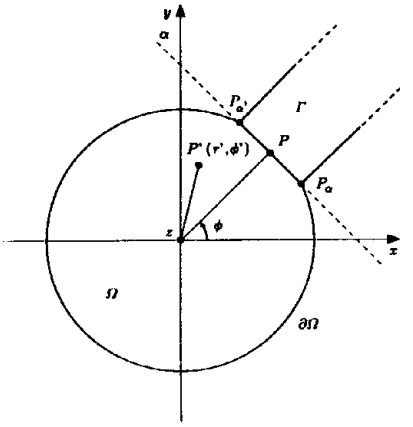

Fig.1 Geometry of the structure.

ϕ_m, and at N frequencies, ν_n, in a given frequency band, $[\nu_a,\nu_b]$. The radiometer equation for the case of discrete data is

$$p_{nm} = \int_\Omega W_{nm}(P')\, T(P')\, dP' \quad , \tag{3}$$

where p_{mn} is an element of $\mathbf{p}$, a vector of $\mathbb{R}^{MxN}$, and $W_{nm}=W(\phi_m,P',\nu_n)$. We are interested in a solution to (3) which is continuous in Ω and vanishes on $\partial\Omega$.

A suitable inner product between elements $\mathbf{p}$ and $\mathbf{q}$ of the image space of $\mathbb{R}^{MxN}$ can be defined by means of the equation

$$(\mathbf{p},\mathbf{q}) = \mu \sum_{n=1}^{N} \sum_{m=1}^{M} p_{nm} q_{nm} \tag{4}$$

where $\mu=(N-1)^{-1}(M-1)^{-1}$. It has been shown [Bardati *et al*, 1991 a; Bardati *et al*, 1991 b] that a suitable scalar product in the object space $X\psi$ of physical temperature is the following

$$(u,v)_{X\psi} = \int_\Omega K(P')\, \nabla u(P') \cdot \nabla v(P')\, dP' \tag{5}$$

where K has the meaning of a thermal conductivity, while u and v are two elements of $X\psi$. To obtain a solution for T from equation (3) in the space equipped by the scalar product (5), we must consider thermal functions $\Psi_{nm}(P')$ such that, for any T(P'):

$$(\Psi_{nm},T)_{X\psi} = \int_\Omega W_{nm}(P')\, T(P')\, dP' \tag{6}$$

Equation (6) enforces T to be the weak solution of

$$-\nabla\cdot(K\nabla\Psi_{nm}) = W_{nm}(P') \tag{7}$$

which satisfies a homogeneous Dirichlet condition on $\partial\Omega$ [Brezis, 1983]. Therefore the thermal functions are immediately recognized from (7) to be solutions of the classical stationary heat equation in Ω vanishing on the boundary.

Finally, solutions for T in the Sobolev subspace spanned by the above defined thermal functions are obtained by enforcing

$$(\Psi_{nm},T)_{X\psi} = p_{nm} \quad , \tag{8}$$

for n=1,...,N and m=1,...,M. It is of interest, and will be done in the following, to compare solutions to (3) in $X\psi$ to those which can be obtained in the object space equipped by the familiar $\mathbb{L}_2$ scalar product:

$$(u,v)_{X_W} = A^{-1} \int_\Omega u(P')\, v(P')\, dP' \quad , \tag{9}$$

where A= mis (Ω). The integral equation obtained by using (9) instead of (5) is similar to equation (8) where, however, we find AW_{nm} instead of Ψ_{nm}.

We look, now, for the minimal-norm solution of equation (8) which can be written in terms of the singular system [Bertero *et al*, 1985] of the integral operator $\mathfrak{T}$, which is defined as

$$(\mathfrak{T}u)_{nm} = (\Psi_{nm}, u)_{X_\Psi} \quad , \tag{10}$$

where the symbol $(\mathfrak{T}u)_{nm}$ denotes the nm-th component of vector $\mathfrak{T}u$. The adjoint of $\mathfrak{T}$ from (4) is

$$(\mathfrak{T}^*\mathbf{q})\,(P') = \mu \sum_{n=1}^{N} \sum_{m=1}^{M} \Psi_{nm}(P')\, q_{nm} \quad . \tag{11}$$

The singular system is obtained from the solutions to the following shifted eigenvalue problem

$$(\mathfrak{T}u_k)_{nm} = \lambda_k\, (\mathbf{q}_k)_{nm} \quad , n=1,...,N;\ m=1,...,M; \tag{12}$$

$$(\mathfrak{T}^*\mathbf{q}_k)\,(P') = \lambda_k\, u_k(P') \quad , P' \in \Omega,$$

where λ_k, $u_k(P')$ and $\mathbf{q}_k \in \mathbb{R}^{MxN}$ are called singular values, singular functions and singular vectors, respectively. By using (12) it is easy to show that the singular values are the square roots of the eigenvalues of the symmetrical Gram matrix:

$$[G]_{nm,n'm'} = \mu(\Psi_{nm}, \Psi_{n'm'})_{X_\Psi} \quad . \tag{13}$$

By means of (7), after a short manipulation we obtain

$$[G]_{nm,n'm'} = \mu \int_\Omega \Psi_{nm}(P')\, W_{n'm'}(P')\, dP' \quad . \tag{14}$$

The singular values are ordered according to $\lambda_k > \lambda_{k+1}$. The singular vector $\mathbf{q}_k$ is the eigenvector of [G] corresponding to λ_k which is normalized according to the norm induced by (4). Finally, the singular functions are obtained from the second equation of (12). The singular functions form an orthonormal basis of X_Ψ, while the vectors $\mathbf{q}_k$ are an orthonormal basis of the image space. It is worth noting that orthonormality must be referred to the inner products (4) and (5).

The temperature is basically retrieved by means of the minimal norm solution of the equation (8), which is

$$\hat{T}(P') = \sum_{k=1}^{NxM} \frac{1}{\lambda_k} (\mathbf{p}, \mathbf{q}_k)\, u_k(P') \quad , \tag{15}$$

Minimal norm solutions are exact solutions of the radiometric equation in the object space in the absence of noise. When noise is considered, regularized solutions must be used to counteract the lack of continuous dependence of the normal solutions on the data. In this paper we shall use a rectangular filter, that consists of limiting the summation in equation (15) to an integer $\Lambda \leq (MxN)$. Such a regularized solution will be denoted by $\hat{T}^{(\Lambda)}$.

The norm $[(\mathbf{p},\mathbf{p})]^{\frac{1}{2}}$ is called *signal* and denoted by $\bar{S}$ in the following. The *channel* noise, δp_{nm}, is commonly defined as the rms value (averaged over the radiometer integration time) of the fluctuation superimposed on the datum measured at frequency ν_n and position ϕ_m, i.e. p_{nm}. The norm $[(\delta\mathbf{p},\delta\mathbf{p})]^{\frac{1}{2}}$ is called *noise* and is denoted by $\bar{N}$. A common definition of degrees-of-freedom of a measurement is the number of independent pieces of information which can be extracted from data in the presence of noise. It can be shown that a reasonable estimate of the number of degrees-of-freedom [Pike *et al*, 1984] of a temperature retrieval by means of (15) is the largest integer Λ' for which the quotient $\lambda_{\Lambda'}/\lambda_1$ is less than the signal-to-noise ratio $\bar{S}/\bar{N}$.

3. Numerical analysis

In this paper the antenna has been modelled as a parallel-plate waveguide, filled by a dielectric material of uniform relative permittivity $\epsilon_r = 30$. To a first approximation cylindrical segments of human body such as limbs and thighs can be described by two concentric cylinders. Therefore the body has been assumed to be composed of two materials, a bone for $r<r_B$ and a muscle for $r_B<r<r_M$. The complex permittivity $\epsilon(P',\nu)$ takes different values in bone and muscle. They will be denoted by ϵ_{Bn} and ϵ_{Mn} in the respective regions, at frequency ν_n. A microwave radiometer equipped by N=4 channels (1.1, 2.5, 4.5 and 5.5 GHz) has been considered in the numerical examples.

It is known from reciprocity in antenna theory that the weighting function is equal to the power deposition within Ω when the antenna is used in the active mode to radiate unitary power into the body. Therefore, at frequency ν_n

$$W_{nm}(P') = - C_{nm}\,\pi\,\nu_n\,\mathrm{Im}\,[\epsilon_n]\,\left|E_{nm}(P')\right|^2 \qquad (16)$$

where C_{nm} is found by imposing condition (2) and $E_{nm}(P')$ is the electric field vector generated by the microwave incident radiation from the antenna at ϕ_m. The minus sign in (16) is due to the fact that the imaginary part of ϵ_n is negative for a time-dependence $\exp(j2\pi\nu_n t)$ of the electromagnetic field, where j is the imaginary unit. Note that E_{nm} and ϵ_n are the only functions defined in $\mathbb{C}$.

The computation of E_{nm} has been performed numerically by a finite-difference time-domain technique [Yee, 1966]. The incident electric field has been assumed as $\hat{\mathbf{z}}\cos(\pi\xi/w)$, $|\xi| \le w/2$, ($\hat{\mathbf{z}}$ is the unitary vector along the z-axis, ξ is the transversal coordinate on the xy-plane of a cartesian frame ξ,η,ζ solidal with the waveguide, and w is the width of the waveguide) at a depth inside the waveguide, where high-order modes, which originate on the aperture, sufficiently vanish. Contour level plots of the weighting functions at radiometer frequencies are shown in Figs. 2-5. It is worth mentioning that, due to the rotational symmetry of the assumed permittivities, the weighting functions depend on the angular difference ϑ between the source point and the angle-of-view ϕ_m : $\vartheta=\phi'-\phi_m$. Moreover, since the tangential electric field is continuous across two media of different permittivities, as a consequence of (16) the weighting functions are also discontinuous.

The thermal functions have been numerically calculated by means of equation (7), where K takes different constant values, K_B and K_M, in bone and muscle. Also for this computation a finite-difference time-domain method has been used, i.e., the term $\partial T/\partial t$ has been added to the left-hand side of (7) and the resulting time-dependent heat-equation has been numerically solved. The steady-state solution is coincident with the solution to (7). Diagrams of the thermal functions are recorded in Figs. 6-9.

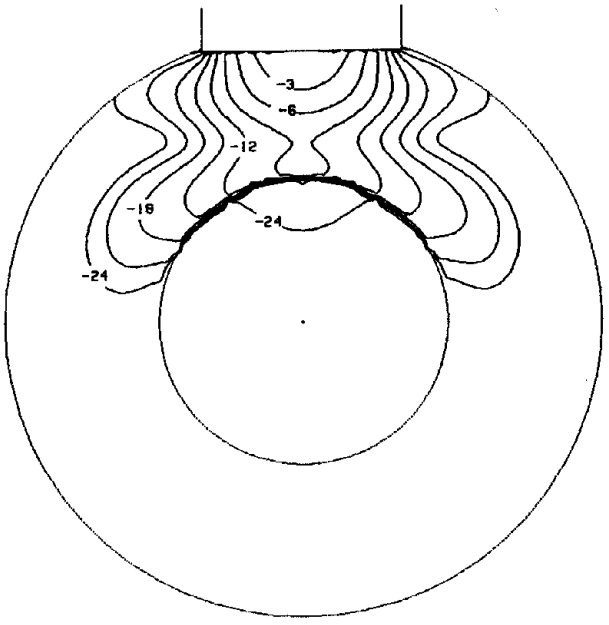

Fig.2 Contour plot of the weighting function at 1.1 GHz. Levels (dB) are referred to a maximum value on the aperture. The size of the grid used for finite-difference computation is 0.1cm. The numerical values used are: r_B=2.8cm, r_M=6.0cm, ϵ_B=6.4-j1.6, ϵ_M=50.5-j24.3.

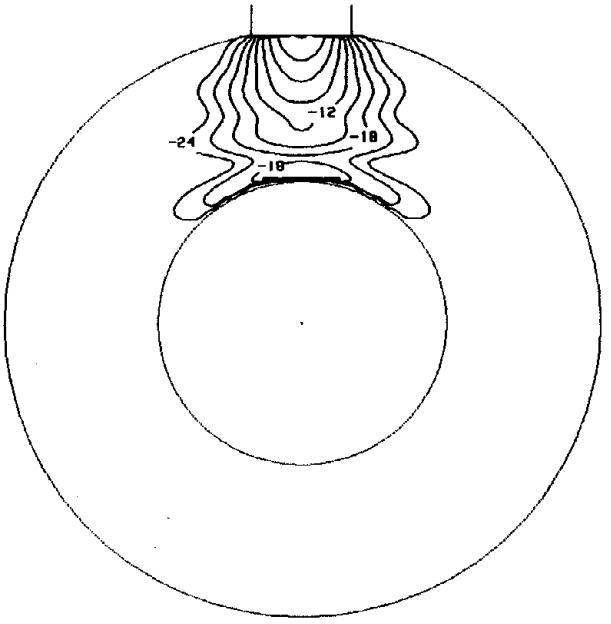

Fig.3 Contour plot of the weighting function at 2.5 GHz.

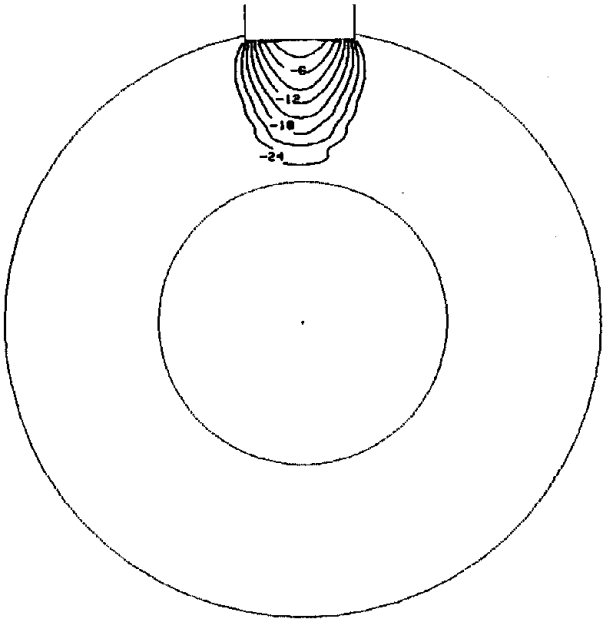

Fig.4 Contour plot of the weighting function at 4.5 GHz.

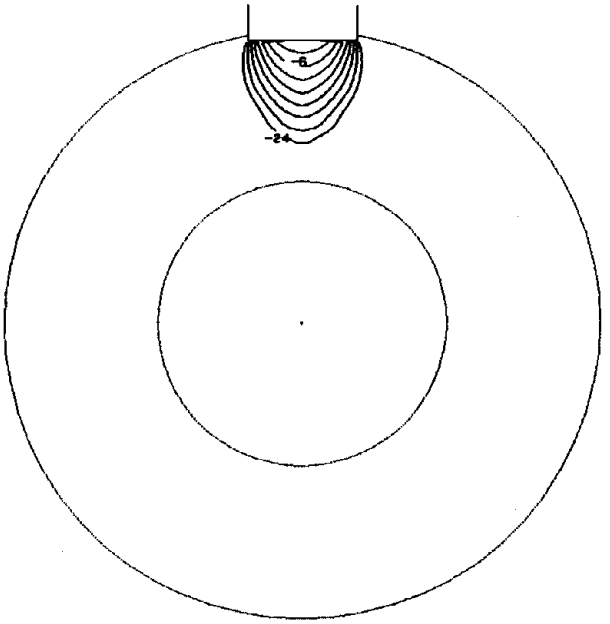

Fig.5 Contour plot of the weighting function at 5.5 GHz.

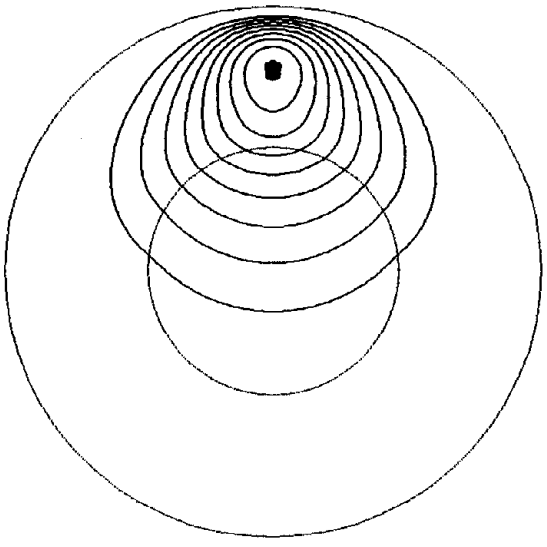

Fig.6 Thermal function Ψ_1. The contour levels are at intervals of 10% of the maximum value. The ratio K_B/K_M=0.74 has been used.

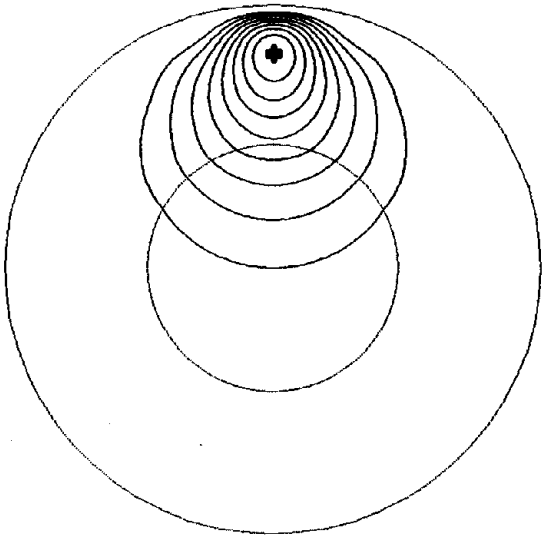

Fig.7 Thermal function Ψ_2.

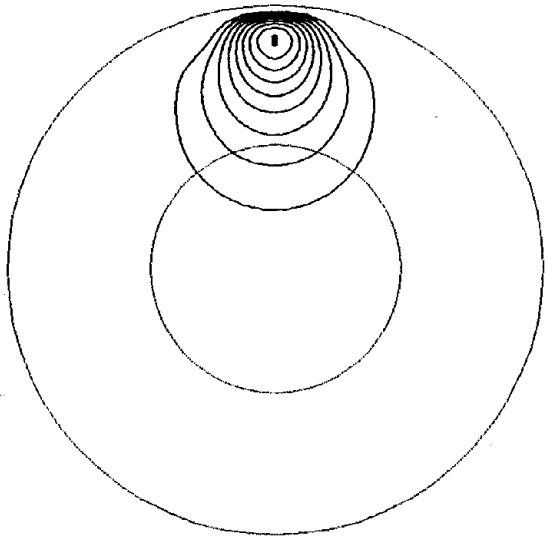

Fig.8 Thermal function Ψ_3.

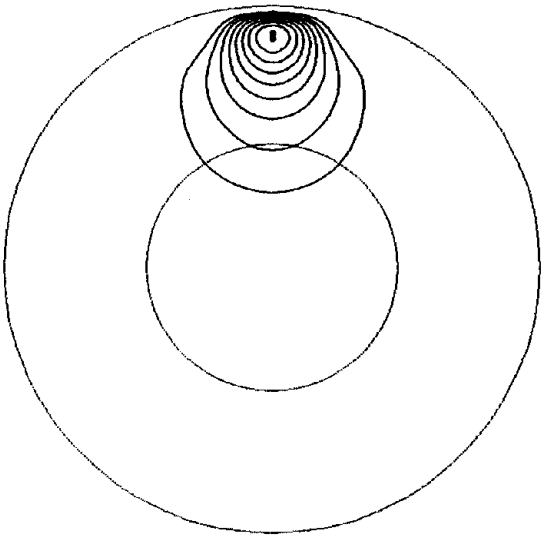

Fig.9 Thermal function Ψ_4.

Let $\mathfrak{C}(e,r_c)$ be a circle fully contained in the annular muscle region $r_B<r<r_M$, of eccentricity e and radius r_c (Fig.10). We have numerically investigated retrievals of temperature functions defined as:

$$T(P') = 1,\ P' \in \mathfrak{C}; \qquad T(P') = 0,\ P' \notin \mathfrak{C}. \tag{17}$$

The above defined functions have been considered for modelling a localized hot spot in a uniform temperature field as may be the case during hyperthermia treatments. Synthetic data have been generated by substituting T(P') from (17) into equation (3) and by letting the antennas assume M=32 equiangular positions around the cylinder. Examples of reconstructions, i.e. contour level plots of $\hat{T}^{(\Lambda)}$, are shown in Figs. 11-16, for various values of e and two values of Λ.

A common feature of retrievals is distortion, in the sense that the sharp original function (17) is retrieved as a main lobe, which corresponds to the maximum of $\hat{T}^{(\Lambda)}$, while secondary lobes can occur (Fig. 11). Moreover a shift of the main lobe maximum with respect to the original function is present. A larger value of Λ, i.e. of the number of terms retained in the minimal norm solution (15), corresponds to an assumed larger ratio S/N. As can be seen from the diagrams, increasing Λ improves the retrievals by reducing the shift and increasing the main lobe sharpness.

A retrieval in the $\mathbb{L}_2$ subspace, X_W, spanned by the weighting functions is shown in Fig. 17 for a comparison with the retrieval in X_Ψ for the same signal-to-noise ratio. The retrieval in X_W exhibits discontinuities as a consequence of the discontinuities of the weighting functions at the boundary between two materials of different permittivities. Moreover a spurious lobe occurs close to the boundary $\partial\Omega$ where temperature is sensed by antennas. This lobe is due to the fact that the weighting functions reach the largest values in the vicinity of the antennas.

4. Conclusions

The problem of the retrieval of a 2D temperature distribution in a circular cylinder observed through a parallel-plane waveguide whose walls are parallel to the cylinder axis has been studied. The retrieval of temperature has been modelled as an inverse problem, whose solution has been investigated in a space spanned by thermal functions.

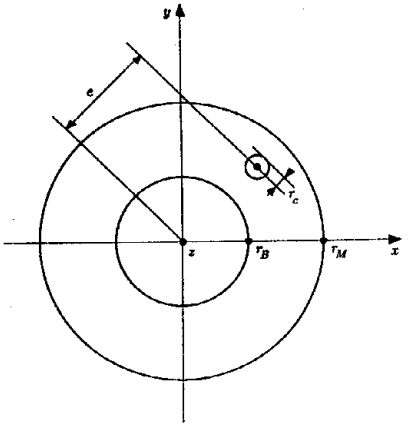

Fig.10 Thermal structure to be radiometrically retrieved for various values of the eccentricity e. The radius of the circular hot spot is r_c=0.5cm.

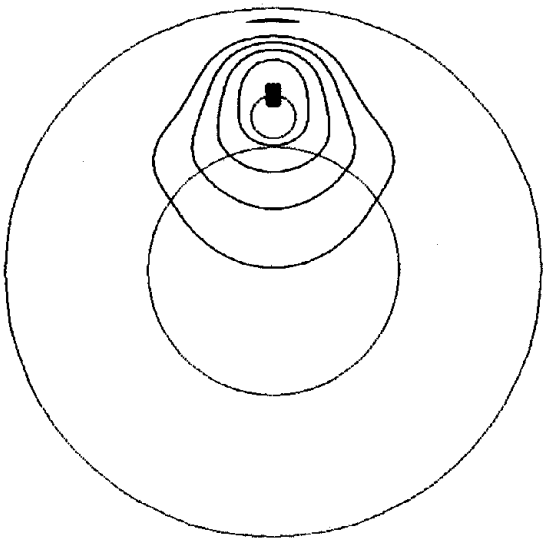

Fig.11 Temperature retrieval, $\hat{T}^{(\Lambda)}$, for e=3.5cm and Λ=27. The value of Λ corresponds to S/N=30. The contour levels are at intervals of 20% of the maximum positive value. Black shaded areas correspond to regions where the retrieved temperature is not less than 98% of the maximum value.

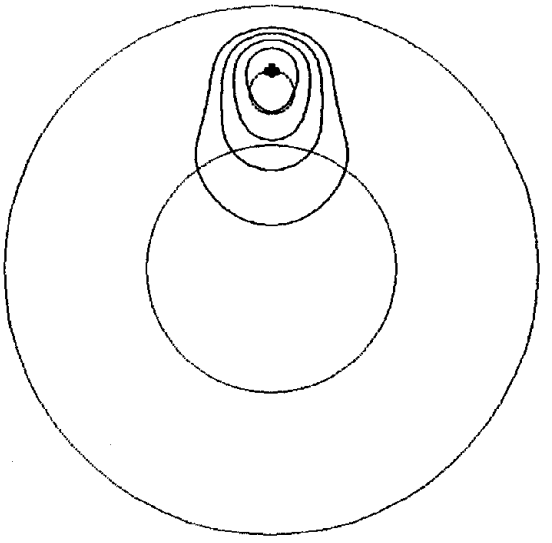

Fig.12 Temperature retrieval, $\hat{T}^{(\Lambda)}$, for e=4.0cm and the same Λ as in Fig.11.

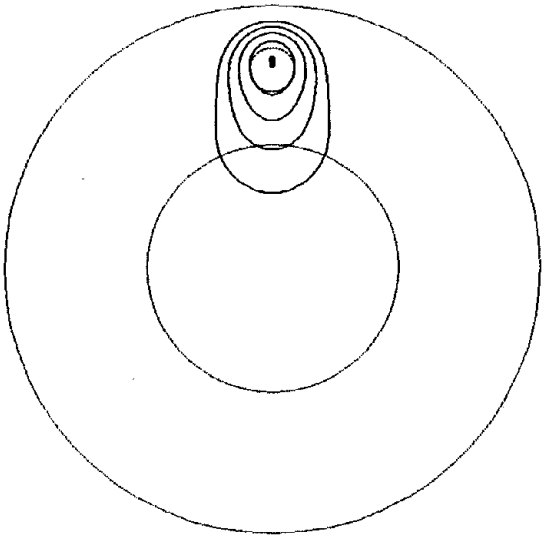

Fig.13 Temperature retrieval, $\hat{T}^{(\Lambda)}$, for e=4.5cm and the same Λ as in Fig.11.

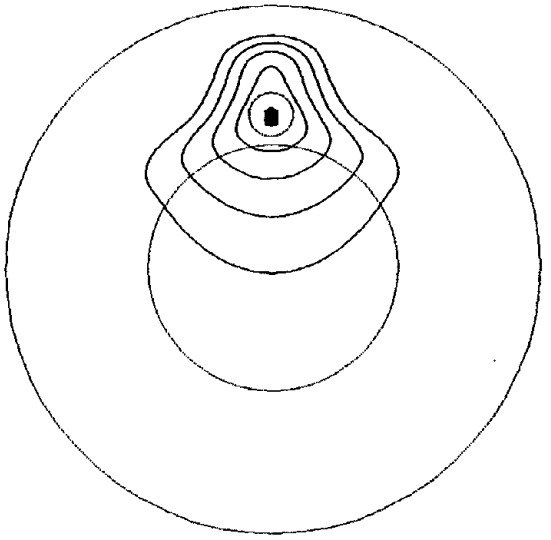

Fig.14 Temperature retrieval, $\hat{T}^{(\Lambda)}$, for e=3.5cm and S/N=100 (Λ=45).

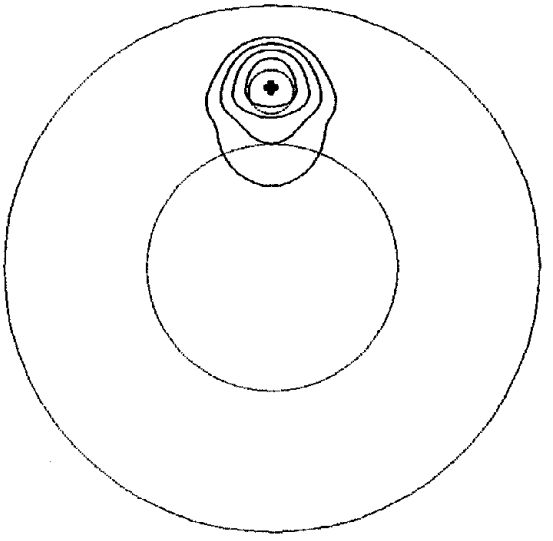

Fig.15 Temperature retrieval, $\hat{T}^{(\Lambda)}$, for e=4.0cm and the same Λ as in Fig.14.

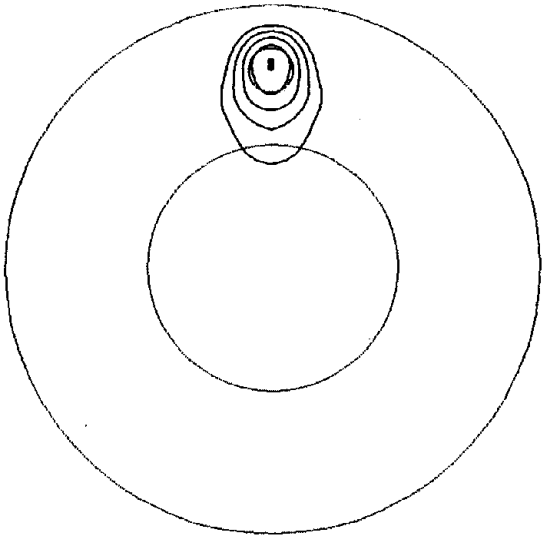

Fig.16 Temperature retrieval, $\hat{T}^{(\Lambda)}$, for e=4.5cm and the same Λ as in Fig.14.

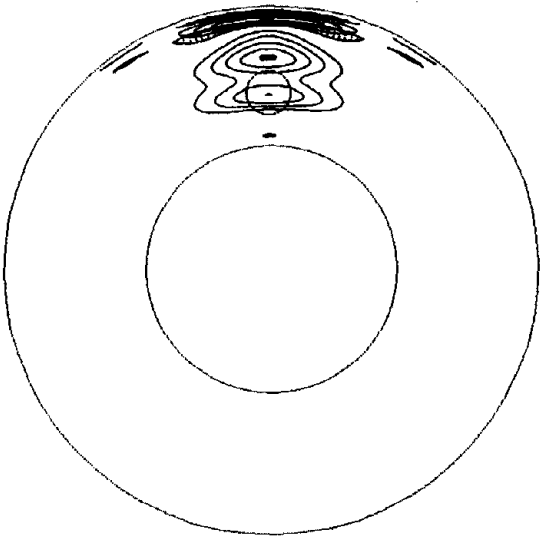

Fig.17 Temperature retrieval, $\hat{T}^{(\Lambda)}$, for e=4.0cm and Λ=44, in the L_2- subspace, X_W, spanned by the weighting functions. The value of Λ corresponds to S/N=30. The same values of e and of S/N have been used for the retrieval (in X_Ψ) shown in Fig. 12. The negative portion of diagrams are indicated by gray shading.

The solution to the inverse problem needs the solutions to two direct problems, an electromagnetic scattering problem and a heat-balance one. In this paper both problems have been numerically solved by finite-difference time-domain schemes of computation. It is worth noticing that also the computation of the temperature distributions due to electromagnetic heating in hyperthermia is commonly performed by numerical procedures which first solve an electromagnetic boundary value problem and then a heat transfer equation. The finite-difference time-domain technique is widely used. Therefore the retrieval of temperature from radiometric data can benefit from numerical techniques which are developed for planning hyperthermia treatments.

Finally the results show that the use of a Sobolev space greatly improves the retrievals.

REFERENCES

F. Bardati and D. Solimini (1983) Radiometric sensing of biological layered media, Radio Sci., 18, 1393-1401.

F. Bardati, M. Bertero, M. Mongiardo, and D. Solimini (1987) Singular system analysis of the inversion of microwave radiometric data: applications to biological temperature retrieval, Inverse Problems, 3, 347-370.

F. Bardati and V.J. Brown (1991 a) Thermal imaging by microwave radiometry, in *Inverse Problems in Scattering and Imaging*, Eds. M. Bertero and E.R. Pike, Adam Hilger, Bristol, pp. 293-318.

F. Bardati, V.J. Brown and P. Tognolatti (1991 b) A useful scalar product in the inversion of radiometric data, in *Italian Recent Advances in Applied Electromagnetics*, Eds. G. Franceschetti and R. Pierri, Liguori, Naples, pp. 151-165.

M Bertero, C De Mol, and E R Pike (1985) Linear inverse problems with discrete data. I: General formulation and singular system analysis, Inverse Problems, 1, 301-330.

B. Bocquet, A. Mamouni, H. Hochedez, J.C. Van deVelde, and Y. Leroy (1986) Visibility of local thermal structures and temperature retrieval by microwave radiometry, Electron. Lett., 22, 120-122.

H Brezis (1983) Analyse functionnelle - Théorie et applications, Masson, Paris.

M. Chive, M. Plancot, G. Giaux, and B. Prevost (1984) Microwave hyperthermia controlled by microwave radiometry: technical aspects and first clinical results, J. Microwave Power, 19, 233-241.

M. Miyakawa (1981) Study on microwave thermography - Application to the estimation of subcutaneous temperature profiles, Trans. Inst. Electr. Comm. Eng. Jpn., E64, 786-792.

S. Mizushina, Y. Hamamura, and T. Sugiura (1986) A Three-band radiometer system for noninvasive measurement of the temperature at various depths, 1986 IEEE-S Int. Symp. Dig., 759-762.

E.R. Pike, J.G. McWhirter, M. Bertero, and C. De Mol (1984) Generalized information theory for inverse problems in signal processing, IEE Proc., 131, 660-667.

K.S. Yee (1966) Numerical solution of initial boundary value problems involving Maxwell's equations in isotropic media", IEEE Trans. Antennas and Propagation, AP-14, 302-307.

ACKNOWLEDGEMENTS

Stimulating discussion with Professor Mario Bertero is gratefully acknowledged.
Partial financial supports by the Ministero dell'Università e della Ricerca Scientifica and the National Research Council of Italy are also acknowledged.